

Modeling Longitudinal Evolution of Decommissioned Geostationary Satellites using Neural Networks

İbrahim ÖZ^{1*}, Cevat ÖZARPA²

¹ Ankara Yıldırım Beyazıt Üniversitesi, TTO, Ayvalı Mah. Ankara, Türkiye

² Ankara Medipol Üniversitesi, Mühendislik Fakültesi, Ankara, Türkiye

*1 ibrahimoz@gazi.edu.tr, ² cevat.oraropa@ankaramedipol.edu.tr

(Geliş/Received: 09/01/2024;

Kabul/Accepted: 27/03/2024)

Abstract: This study uses neural networks to explore the intricate longitudinal progression of decommissioned geostationary satellites. The goal is to model and predict satellites' longitudinal dynamics across time dimensions. Historical satellite longitude data undergoes thorough preprocessing to train time series neural networks in both single-input and 3-input configurations for all six decommissioned satellites, yielding comprehensive longitudinal behavior insights. Results reveal impressive outcomes: average Mean Squared Error (MSE) between predicted and measured longitudes is 1.55×10^{-3} , with regression close to unity. This convergence implies a strong alignment between the neural network methodology employed and the intricate problem domain. These results accentuate the suitability and effectiveness of the chosen neural network approach in addressing the challenges posed by decommissioned geostationary satellite trajectory modeling. The study's implications span various fields. Insight into long-term orbital shifts aids in understanding satellite behaviors, enhancing trajectory predictions and decision-making in satellite management and space technology advancement. Additionally the research emphasizes the importance of accurate predictions about satellite behavior after decommissioning. This contributes to better mission planning, resource optimization, and more efficient strategies for dealing with space debris.

Key words: Decommissioned satellites, geostationary orbits, neural networks, longitudinal evolution, orbit dynamics.

Ömrünü Tamamlamış Yer Sabit Uyduların Boylam Hareketlerinin Yapay Sinir Ağları ile Modellenmesi

Öz: Bu çalışmada, yapay sinir ağları kullanılarak işletme ömrünü tamamlamış yer sabit yörünge uydularının boylam hareketleri incelenmiştir. Uydu yörünge hareketleri ve dinamiği içinde, uydu boylam hareketleri yapay sinir ağları ile modellenmiştir. Ömrünü tamamlamış altı uyduya ait veriler, veri tabanından alınmış, kapsamlı bir ön işleme tabi tutulmuş ve hem tek girişli hem üç girişli yapay sinir ağı eğitiminde kullanılmıştır. Modelleme sonunda ölçülen ve tahmin edilen sonuçlar arasındaki ortalama kare hata (MSE) 1.55×10^{-3} ve regresyon değeri 1 civarında olup tüm uydular için oldukça başarılı sonuçlar elde edilmiştir. Böylece yapay sinir ağları ile karmaşık yörünge dinamiğinin modellenebildiği görülmüştür. İşletme ömrünü tamamlamış uyduların boylam hareketlerinin yapay sinir ağları ile etkili bir biçimde modellenebildiği görülmektedir. Uydu operatörleri bu tip uyduların uzun vadeli yörünge hareketlerini önerilen yöntem ile tahmin edebilir ve tahminlerini bu konuda alacakları kararlar için destek bilgisi olarak kullanabilir. İlave olarak bu araştırma ömrünü tamamlamış uyduların hareketlerini hassas bir şekilde göstermekte bu durumda daha iyi görev planlaması yapmaya, kaynak optimizasyonuna ve uzay enkazlarının daha iyi yönetilme stratejilerinin geliştirilmesine imkân tanımaktadır.

Anahtar kelimeler: Ömrünü tamamlamış uydu, yer sabit yörünge, yapay sinir ağları, boylam değişimi, yörünge dinamiği.

1. Introduction

Fırat Geostationary satellites gracefully encircle the earth at an unwavering 35,786 km altitude above the equator. This exceptional orbital position, synchronized with the earth's rotation, facilitates straightforward ground-based tracking. The stability of this position proves invaluable for television, data communication, and other applications that benefit from consistent connectivity. The 24-hour orbital period ensures uninterrupted communication, allowing antennas to remain aligned with GEO satellites, transmitting and receiving signals without needing constant adjustments [1-2].

The orbit raising of a geostationary satellite's operational life is marked by the exhaustion of its onboard fuel reserves. At this critical juncture, the satellite's maneuverability is significantly compromised, and its ability to perform controlled orbital adjustments diminishes. Consequently, a carefully orchestrated decommissioning process is initiated to manage the satellite's fate and ensure the long-term sustainability of the space environment.

* Sorumlu yazar: ibrahimoz@gazi.edu.tr. Yazarların ORCID Numarası: ¹ 0000-0003-4593-917X, ² 0000-0002-1195-2344

The International Telecommunication Union (ITU), a specialized agency of the United Nations, plays a pivotal role in space communication governance. ITU's Radio Regulations (RR) provide a framework for managing orbital slots and frequency assignments, ensuring interference-free communication services. The regulation Rec. ITU-R S.1003 of the ITU R pertains to the disposal of space systems, particularly geostationary satellites, once they cease their operational activities due to fuel depletion or other reasons. According to this regulation, satellite operators are mandated to remove their satellites from the geostationary orbit at the end of their mission [3-4].

Similarly, The Inter-Agency Space Debris Coordination Committee (IADC) advises measures to mitigate space debris, including preventing break-ups, relocating spacecraft and orbital stages after missions, and limiting object releases. For geostationary satellites at the end of their operational life, recommendations include relocating them from the crowded geostationary orbit region and passivating them to reduce explosion risks, though this passivation can influence their orbital characteristics. These steps collectively aim to reduce debris and uphold space environment sustainability [5-6].

Geostationary satellites (GEO satellites) are typically decommissioned within the range of 150 km to 500 km above the geostationary belt. Once a decommissioned satellite is placed in its new graveyard orbit, its orbital behavior is influenced by several factors, including the earth's gravitational pull, solar wind, and gravitational forces from other celestial bodies. These perturbations introduce variations in the satellite's orbital elements over time, which can be categorized into three main types: short-periodic, long-periodic, and secular terms. Short-periodic variations terms of a satellite impact elements like semi-major axis, eccentricity, inclination, ascending node, and argument of perigee. They arise from perturbations with periods less than one year, including earth's non-spherical mass distribution, the moon's and Sun's gravitational effects, and solar radiation pressure. These variations can lead to daily or monthly changes in orbital elements. Long-periodic variations affect the same orbital elements, arising from perturbations with periods exceeding one year, such as the gravitational influence of the moon and Sun and solar radiation pressure. These variations cause changes on a yearly or multi-year basis.

In the realm of artificial intelligence (AI) and machine learning (ML), a plethora of methodologies and applications have emerged, showcasing the immense potential and versatility of these technologies. Methodologically, AI and ML encompass a wide spectrum of techniques, including feature selection and stability analysis [7], hybrid control systems involving artificial neural networks (ANNs) and fuzzy PI control [8], and comparative assessments of predictive algorithms, such as ordinary ANNs and convolutional neural networks (CNNs) for customer churn prediction [9]. These methods collectively form the foundation for addressing complex challenges across diverse domains.

When it comes to real-world AI applications, the breadth of possibilities is striking. AI-driven techniques play a pivotal role in forecasting Turkey's natural gas consumption [10], utilizing LSTM-based deep learning methods for earthquake prediction through ionospheric data analysis [11], and improving the precision of daily wind energy predictions through machine learning and statistical techniques [12]. In the healthcare sector, AI comes to the forefront with a machine learning model for diagnosing Type 2 diabetes based on health behavior [13], while in the field of speech recognition, recurrent units like LSTM and GRU find applications in Turkish speech recognition techniques and broader speech processing endeavors [14]. These references represent just a glimpse of the rich tapestry of AI and ML methodologies and applications, each contributing uniquely to their respective domains and expanding the horizons of technological possibilities.

This study focuses on the longitudinal behavior of decommissioned GEO satellites with machine learning over time. Due to the tumbling motion of deorbited GEO satellites, accurately determining their sunlit surface area and surface reflection coefficient proves challenging. Additionally, the dynamic modeling of GEO satellites is complex due to the presence of various perturbing forces [15].

2. Satellite Dynamics in GEO Graveyard Region

Decommissioned satellites exhibit a specific movement known as "drift" in an eastward direction when transitioning to the graveyard orbit. The eastward drift of decommissioned GEO satellites is influenced by a combination of factors, primarily the gravitational perturbations caused by the non-spherical mass distribution of the earth, gravitational forces from the moon and Sun, and solar radiation pressure. While these satellites were initially positioned in a geostationary orbit where their orbital period matched the earth's rotation period, their relocation to the graveyard orbit changes their orbital parameters. [16]

The eastward drift occurs due to the interaction of these perturbing forces. As the satellite moves away from its original geostationary position, the gravitational forces from the moon and Sun and the solar radiation pressure act as external accelerations, causing the satellite's orbit to slowly shift in an eastward direction. This phenomenon can be visualized as the satellite "catching up" with the earth's rotation as it moves along its orbital path. It's important to note that the drift of decommissioned GEO satellites is a natural outcome of the complex interplay

between various gravitational and radiation forces. This phenomenon is well understood and is a critical consideration when planning the end-of-life operations of GEO satellites to ensure their safe disposal and to minimize the risk of collisions with operational satellites in the geostationary region. [17, 18]

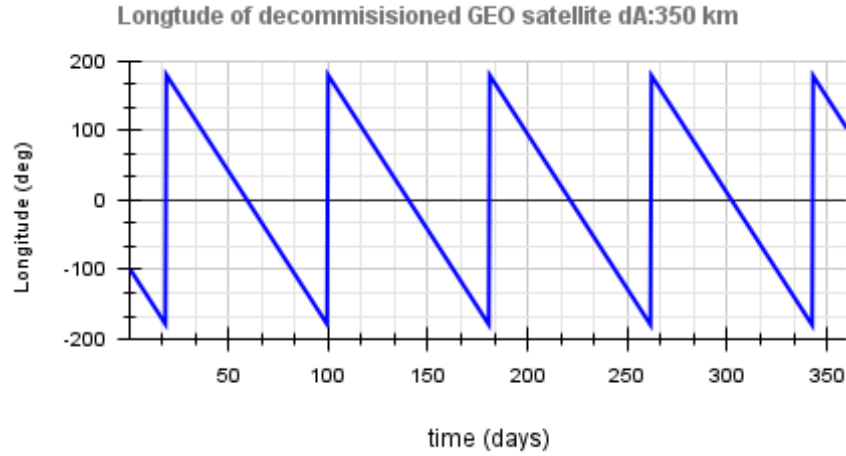


Figure 1. Decommissioned GEO satellite 350 km above the GEO belt, typical longitude values over a time.

The longitude drift rate (D) is highly related to the semi-major discrepancy (Δa) relative to the synchronous semi-major axis a_s , whose value is almost constant subjected to the non-spherical terms of the earth's gravitation field [16].

The daily longitude drift rate can be expressed in Equation 1.

$$D = -\frac{3}{2} \frac{n_c}{a_c} (a - a_c) \frac{1}{n_c} \frac{86400}{86164.09} 360^\circ = -0.0128^\circ (a - a_c) \quad (1)$$

where D : drift rate $^\circ$ / day, a : semi-major axis, a_c : ideal GEO semi-major axis, $n_c = \sqrt{\mu/a_c^3}$

The drift rate is counted positively in the eastward direction. If $\Delta a=0$, then $D=0$. If $\Delta a>0$, then $D<0$, which means that the semi-major axis' increment results in that the satellite rotates slowly relative to the spin of the earth. By contrast, the semi-major axis' decrement results in the satellite running faster than the earth's spin. One kilometer of semi-major discrepancy induces a longitude drift rate of 0.0128 per day.

Table 1 presents the altitudes of decommissioned GEO satellites from GEO ideal orbit 35786 km along with their corresponding relative changes in longitude expressed in degrees per day. The table also includes the duration of one complete revolution around the earth for each altitude.

Table 1. GEO Decommissioning Altitude and Relative Longitude Change

GEO altitude	GEO+150 km	GEO+200 km	GEO+350 km	GEO+500 km
Δ Long ($^\circ$ /day)	-1.92	-2.56	-4.48	-6.40
Revolution Time (days)	187.50	140.63	80.36	56.25

As expected, there is a direct correlation between altitude and the rate of change of longitude per day, with higher altitudes resulting in faster rates of change. Consequently, the time needed a deorbited satellite to complete one full revolution around the earth decreases as its altitude increases. By interpreting these relationships, we can make more accurate orbital predictions and enhance our overall understanding of satellite movements. [19, 20].

2.1 Data Collection and Processing

In this comprehensive study, we have extensively investigated the behavior of six decommissioned geostationary satellites, each identified by their NORAD IDs: Eutelsat-33A (NORAD ID: 27948), Intelsat-801 (NORAD ID :24742), Meteosat-6 (NORAD ID: 22912), Astra-1F (NORAD ID: 23842), Turksat-1B (NORAD ID: 23200), and Turksat-2A (NORAD ID: 26666). Our research primarily focused on analyzing the longitudinal evolution and orbit dynamics of these satellites over time.

We sourced the observed orbital parameters from publicly available information on space track databases to gather essential data for our analysis [21]. These datasets were carefully curated, providing precise and accurate information on each satellite's position, velocity, inclination, eccentricity, and other relevant orbital characteristics.

Table 2 provides the initial data of six satellites, obtained from the publicly available Celestrack data source and based on the epoch of January 1st, 2020, at 9:00 UTC. The orbital parameters listed in Table 2 offer a comprehensive insight into the initial configurations of these decommissioned satellites. These orbital parameters, including Semi-Major Axis (SMA), Eccentricity (Ecc), Inclination (inc), Right Ascension of Ascending Node (RAAN), Argument of Perigee (AoP), True Anomaly (TA), and Longitude (Lon), provide a foundation for analyzing the orbital dynamics and behaviors of these satellites. Such detailed information is invaluable for studying how these satellites interact with the geostationary region and how various factors influence their trajectories over time.

Table 2. The orbital parameters of the six satellites at the designated epoch.

Satellites	SMA	Ecc	inc	RAAN	AoP	TA	Lon
Astra-1F	42585.399	0.001072	7.180	55.865	295.853	14.605	131.309
Eutelsat-33A	42559.163	0.000415	4.418	74.147	189.917	7.313	36.097
Intelsat-801	42602.619	0.001350	8.476	48.262	301.030	331.613	85.710
Meteosat-6	42531.116	0.000370	13.873	18.878	242.078	23.270	48.879
Turksat-1B	42512.006	0.001461	11.492	32.772	33.950	175.002	6.011
Turksat-2A	42754.583	0.001215	3.331	81.888	247.414	133.713	250.428

A comprehensive dataset spanning a period of two years, beginning from the selected epoch, was acquired from the Celestrack database. These data points serve as the foundation for analyzing and modeling the longitudinal behavior of decommissioned geostationary satellites.

Figure 2 offers a graphical representation that emphasizes the positions of decommissioned geostationary satellites, which serve as the primary dataset for the analysis conducted in this study. The figure showcases the longitudinal changes of these satellites, which are expressed in terms of degrees per day. These changes signify the gradual evolution of the satellites' positions along their orbits over time. The data used for this visualization was sourced from the Celestrack database, a reputable repository of orbital information. This dataset, allows us to observe and analyze the patterns of movement exhibited by these satellites during this period. The graphical representation is a valuable tool for visually comprehending the complex orbital dynamics and longitudinal changes these decommissioned satellites undergo in their post-operational phases.

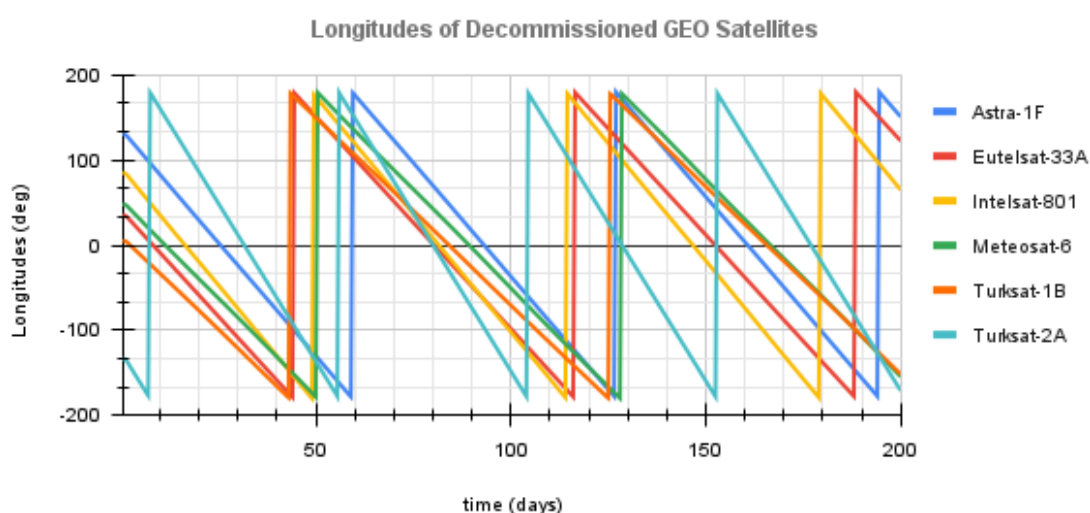


Figure 2. Decommissioned geostationary satellites, accompanied by their respective longitudinal changes expressed in degrees per day.

3. Neural Network Modeling of Decommissioned Satellites

Various forms of neural networks, deep learning, and artificial intelligence are extensively applied across diverse satellite domains, exemplified by various research efforts. Stepišnik et al. explored the utilization of machine learning to enhance spacecraft operation within dynamic radiation environments [22]. Roberts, Solera, and Linares delved into geosynchronous satellite behavior classification via unsupervised machine learning [23]. Supervised machine learning was applied in geosynchronous satellite maneuver classification and orbital pattern anomaly detection [24]. Solera, Roberts, and Linares addressed the geosynchronous satellite pattern of life node detection and classification, presenting their findings at the 9th Space Traffic Management Conference [25]. Roberts and Linares further contributed to the field by focusing on geosynchronous satellite maneuver classification via supervised machine learning at the Advanced Maui Optical and Space Surveillance Technologies Conference. These studies collectively illustrate the broad spectrum of satellite applications enriched by neural network paradigms and artificial intelligence techniques.

Over time, there has been a consistent rise in interest and exploration within artificial neural networks, marking a significant evolution from the early stages of machine learning. This evolution has given rise to one of the most prevalent subsets of artificial intelligence algorithms known as deep learning architectures. Complementary to these architectures, plethora of innovative approaches have emerged within the realm of deep learning, aiming to tackle and solve an array of complex problems in artificial intelligence. These advancements in intelligent solutions have reverberated across an extensive spectrum of sectors, including but not limited to industry, medicine, robotics, image processing, computer vision, object detection, speech processing and recognition, translation, future prediction, finance, and a myriad of other domains [26-28]. This widespread applicability underscores the significance and breadth of impact that artificial neural networks, particularly within deep learning frameworks, have achieved in modern-day AI applications.

In this study, we have developed a neural network model to predict the longitude of six decommissioned geostationary satellites. The model comprises single-input and three-input layers, with a single output layer dedicated to predicting the longitude. The neural network architecture incorporates ten hidden layers, each containing interconnected neurons, and two time delays as shown in Figure 3. This intricate configuration empowers the network to effectively capture and understand the intricate patterns and intricate relationships between orbital dynamics and the resulting variations in longitude. Through this architecture, the neural network learns to discern the complex interplay of factors affecting the longitudinal behavior of these satellites.

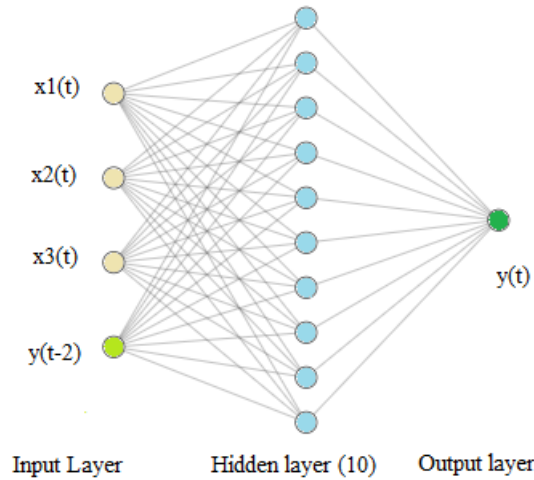


Figure 3. Nonlinear autoregressive neural networks with exogenous Input

Assuming $x(t)$ represent the exogenous input at time t , and $y(t)$ be the output of the network at time t . The network takes into account the historical values of its own output and the exogenous inputs up to the current time to predict the next output. Mathematically, this can be represented through Equation (2),

$$y(t) = f(y(t-1), y(t-2), \dots, y(t-d_y), x(t-1), x(t-2), \dots, x(t-d_x); \theta) \quad (2)$$

where d_y : is the number of lagged terms considered for the output time series, d_x : the number of lagged terms considered for the exogenous input time series, θ : represents the set of all parameters (weights and biases) in the network

The dynamics of the network can be represented for hidden state by the following Equation (3),

$$h(t) = \sigma(W_{hh}h(t-1) + W_{hx}x(t) + b_h) \quad (3)$$

the output prediction can be expressed with Equation (4),

$$y(t) = W_{yh}h(t) + b_y \quad (4)$$

W_{hh} , W_{hx} , and W_{yh} represent the weight matrices associated with the hidden state transitions, exogenous input transitions, and output generation, respectively.

During training, the network learns the weight matrices W_{hh} , W_{hx} , and W_{yh} , as well as the bias vectors b_h and b_y , through optimization techniques such as gradient descent. The objective is to minimize the difference between the predicted output $y(t)$ and the actual target output at each time step. The specific choice of activation functions, network architecture (recurrent neural network), and optimization algorithm selected according to datasets and the problem.

By delving into the interplay between past longitude values and the associated input variables, the network becomes proficient in capturing underlying patterns and correlations. This learning process empowers the network to make accurate predictions about future longitudes. Such predictive capabilities are crucial for comprehending the positioning of satellites in space and facilitating informed decision-making processes.

This comprehensive study involves collecting data spanning a total of 1463 samples for each satellite, which is pivotal for facilitating the training of neural networks to achieve predictive capabilities. The dataset is meticulously divided into three distinct segments: 70% (1025 samples) is allocated for the training phase, 15% (219 samples) for validation, and the remaining portion for rigorous testing. During the training process, the neural network undergoes iterative adjustments in response to computed errors, thus refining its predictive performance. The validation subset evaluates the network's generalization capacity, thereby leading to the termination of training when further improvements in performance plateau. Conversely, the testing subset serves as an independent evaluation mechanism, assessing the network's operational efficiency both during and after the training phase. This approach ensures that the network's performance is rigorously assessed while preserving the integrity of the training process.

As previously outlined, the study encompasses two distinct modes of training: a single input paradigm that exclusively involves day values and a more intricate 3-input framework that encompasses day values, semi-major axis, and latitudinal inputs. This dual-training approach allows the neural network to learn from multiple dimensions of data, enhancing its predictive capabilities and enabling a more holistic understanding of the complex interplay between orbital parameters and longitudinal changes.

The gathered dataset is divided into distinct training and validation sets. The neural network is then subjected to training using the allocated training data, during which it learns to predict longitudes based on input data. This learning process takes place iteratively, refining the model's ability to generate accurate predictions.

The Mean Squared Error (MSE) is employed as a pivotal performance indicator to gauge the effectiveness of the proposed model's predictive performance. The utilization of this metric involves quantifying the accuracy and quality of predictions by assessing the dissimilarity between predicted and actual values. The MSE is mathematically expressed as follows;

$$MSE = \frac{1}{N} \sum_{i=1}^N (y_{measured} - y_{predicted})^2 \quad (5)$$

The MSE metric incorporates the absolute differences between the actual and predicted values. However, through squaring these differences, the emphasis is placed on larger errors, resulting in an average squared difference between the actual and predicted values.

$$R^2 = 1 - \frac{\sum_{i=1}^N (y_{measured} - y_{predicted})^2}{\sum_{i=1}^N (y_{measured})^2} \quad (6)$$

In this research, the Levenberg-Marquardt training algorithm is selected due to its superior performance compared to alternative methods. The training, validation, and testing outcomes assessment relies on two key metrics: Mean Squared Error (MSE) and Regression R Values. The MSE metric quantifies the average squared difference between projected outputs and real targets, with lower values signifying heightened accuracy (zero value indicates no error). The Regression R Values measure the correlation between anticipated outputs and target values, with an R-value of 1 signifying a strong association and a value of 0 denoting a random relationship. By leveraging these evaluation metrics in conjunction with the effective Levenberg-Marquardt training algorithm, our study aims to deliver precise and dependable predictions for estimating the longitude of decommissioned satellites, thereby advancing the capabilities of neural network modeling within this domain.)

4. Results and Discussion

In this study, we delved into the intricate task of modeling the longitudinal evolution of decommissioned geostationary satellites by applying time series neural networks. Our primary objective was to harness neural networks' capabilities to predict these satellites' longitudinal behavior, shedding light on their orbital dynamics and contributing to the advancement of predictive modeling in space science.

Through rigorous data collection and meticulous analysis, we constructed and evaluated a neural network model that effectively captures the complex relationships between past longitudinal values and other relevant orbital parameters. The dataset, spanning 1463 points, was meticulously partitioned into training, validation, and testing subsets, ensuring a robust evaluation of the model's predictive prowess. By employing a 10-layer neural network architecture with interconnected neurons and two delays, we facilitated the network's ability to discern and understand the intricate patterns that govern the longitudinal changes of decommissioned geostationary satellites.

Our investigation encompassed both single-input and 3-input paradigms, wherein we considered the historical data of longitude (y) as well as other pertinent factors (x), such as semi-major axis and latitude. The neural network successfully learned from these input data to accurately predict the longitude variations over time. The model's effectiveness was assessed using performance metrics, namely Mean Squared Error (MSE) and Regression R Values. Our findings highlighted that the Levenberg-Marquardt training algorithm yielded superior results, underpinning the model's capability to provide reliable and precise predictions.

The results from our modeling efforts revealed promising outcomes. The predicted versus measured longitude differences exhibited remarkable accuracy, as evidenced by the low MSE values and regression values of 0.999. This alignment between predictions and actual observations underscores the robustness of our neural network model in capturing the longitudinal evolution of decommissioned geostationary satellites. The model's predictive capability holds significant implications for satellite operators and space agencies, enabling better mission planning, decision-making, and resource allocation during the post-operation phases of satellite lifecycles.

An individual neural network model has been established and trained for each satellite in two distinct scenarios: single-input and three-input cases. The outcomes encompass both predicted longitudes and associated errors, signifying the disparities between the predicted and measured values. Among multiple time response graphs illustrating satellite behavior, particular attention has been given to Eutelsat's results to avoid redundancy. In Figure 4, the graphical representation showcases the alignment of measured and predicted longitude values for Eutelsat-33A. The congruence between the two sets of values is evident, with negligible divergence. The lower segment of the figure exhibits the variance between the two, demonstrating an error fluctuating within the range of ± 0.05 degrees. This exceptional error magnitude underscores the remarkable performance and accuracy of the neural network modeling employed.

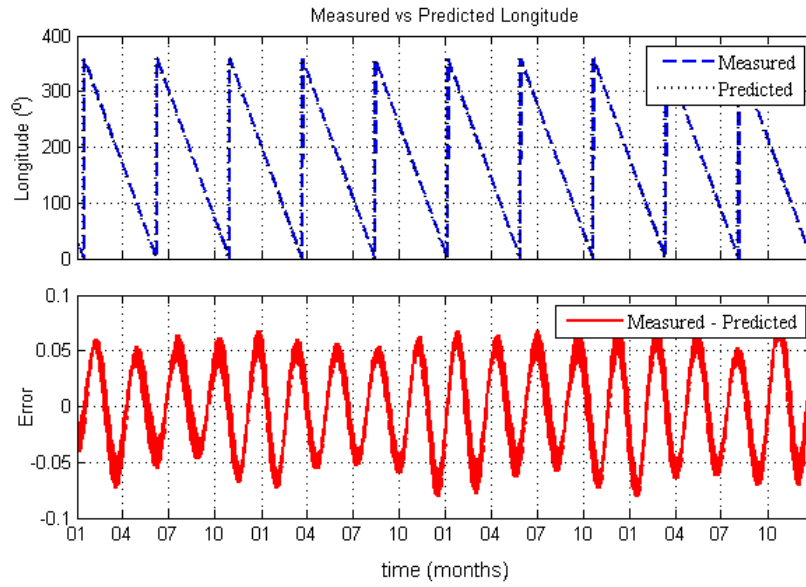


Figure 4. Eutelsat-33A: Measured and Predicted Longitude Values (Upper) and Differences (Lower)

Figure 5 offers an insightful representation of the dynamics of Mean Squared Error (MSE) in conjunction with the number of iterations during the iterative modeling procedure. This depiction is presented on a logarithmic scale for four specific satellites: Eutelsat-33A, Intelsat-801, Meteosat-6, and Turksat-2A. As anticipated, the errors consistently diminish as the iterative process advances. This pattern is consistent with the expected trajectory of iterative optimization algorithms commonly employed in neural network training. The gradual decrease in errors across successive iterations signifies the model's iterative refinement of predictions. Through this incremental learning process, the neural network adeptly hones its predictions, leading to a significant reduction in MSE and a heightened precision in estimating longitudes.

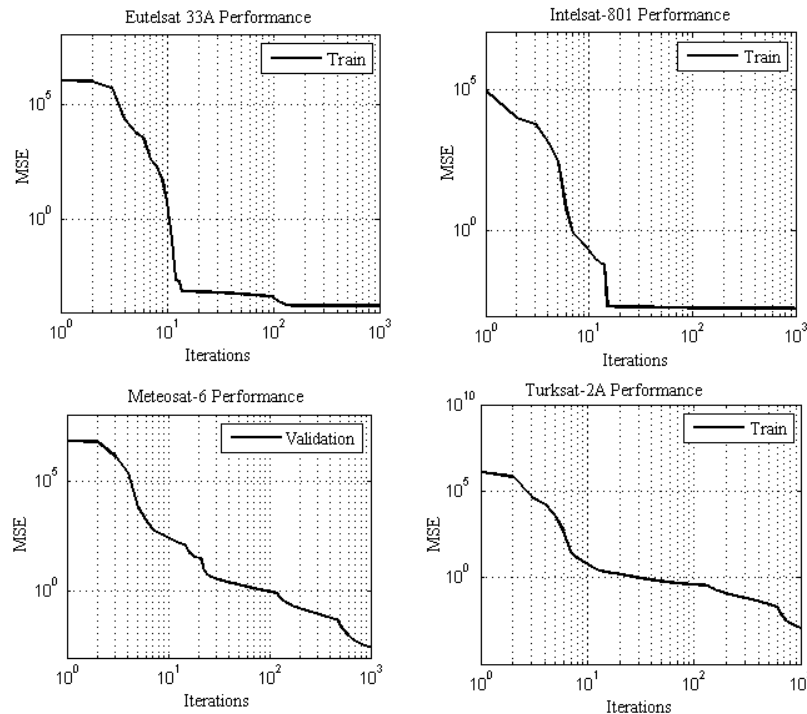


Figure 5. Mean Squared Error (MSE) Performance of Neural Network Across Iterations for 4 Satellites

Figure 6 illustrates a comprehensive juxtaposition between the measured and predicted longitudes regression for four satellites: Eutelsat-33A, IS-801, Meteosat-6, and Turksat-2A. Remarkably, the data points congregate closely along the 45-degree line, signifying a substantial correlation between the predicted and observed longitudes. The quantitative metrics further underscore the model's efficacy. The regression value (R) demonstrates an exceptional score of 0.9999, underscoring the robust and meaningful relationship between the predicted and measured data points.

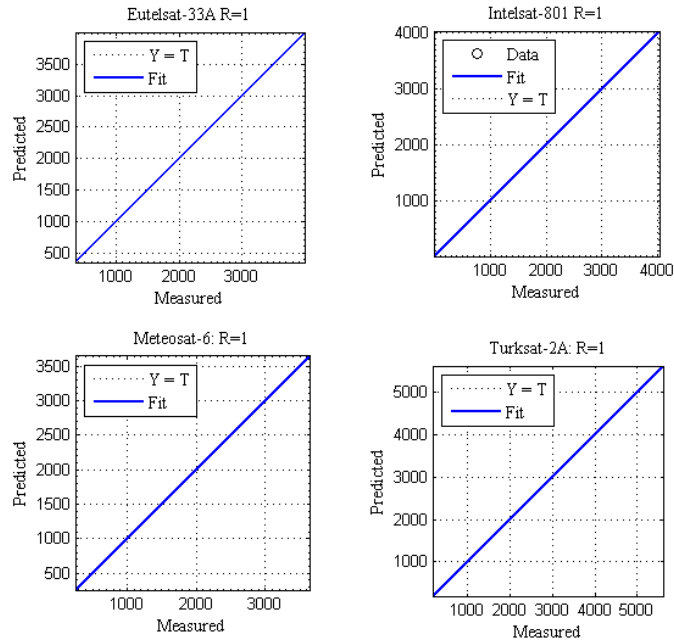


Figure 6. Regression Analysis of Predicted vs. Measured Longitudes for Four Decommissioned Satellites

Figure 7 provides a comprehensive visualization of the discrepancies between measured and predicted values for all six satellites, each represented by distinct colors as indicated in the legend. The x-axis represents the passage of time in months over a span of two years, while the y-axis depicts the magnitude of errors, which varies for each satellite. Despite the distinct amplitudes of these errors, it is notable that all error values remain consistently low across the board. This collective observation serves as a strong testament to the efficacy and accuracy of the employed modeling approach.

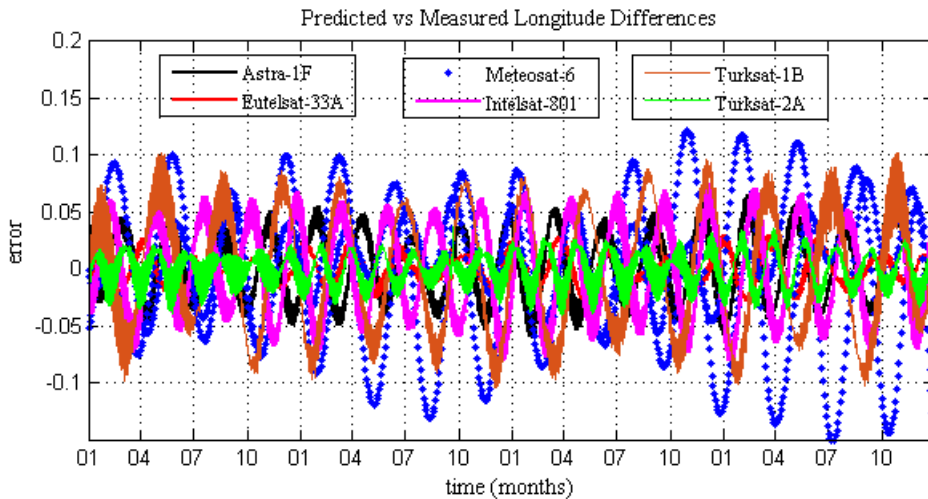


Figure 7. Comparison of Measured and Predicted Longitude Differences over 24 Months for All Six Decommissioned Satellites

Figure 8 offers an enhanced perspective by zooming in on the details of Figure 7, specifically focusing on a 3-month timeframe for all satellites, namely Astra-1F, Eutelsat-33A, Meteosat-6, Intelsat-801, Turksat-1B, and Turksat-2A. Notably, the sine wave ripples observable in the graph are attributed to the influence of eccentricity and other external factors such as the sun and the moon that influence the satellite orbits. These ripples exhibit distinct patterns for each satellite due to their unique orbital characteristics. Remarkably, the error values associated with these predictions remain consistently small, underscoring the precision and effectiveness of the modeling approach employed in this study.

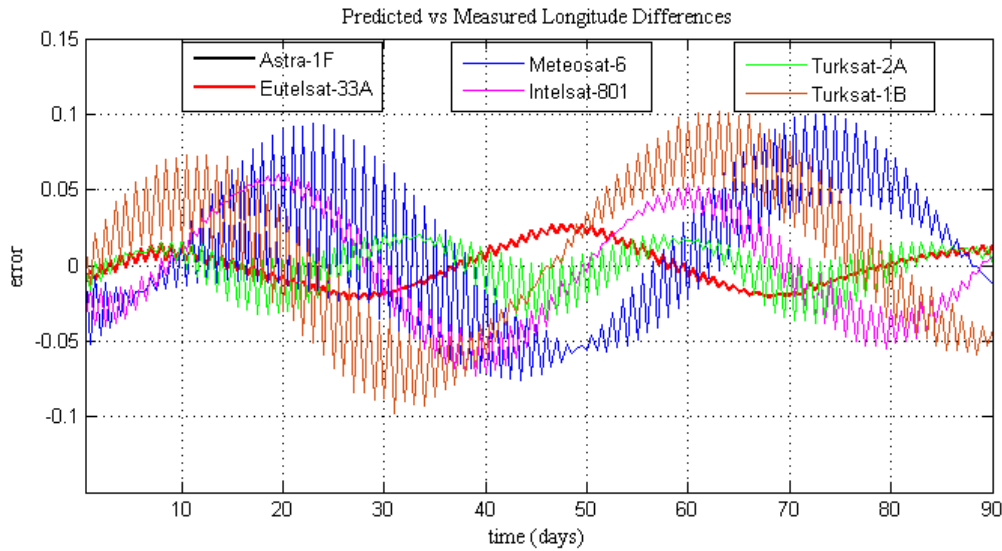


Figure 8. Zoomed-in Three-Month Comparison of Predicted vs Measured Longitude Differences for All Six Satellites

Table 2 furnishes a comprehensive comparison of the anticipated and observed variations in satellite longitudes and the accompanying Mean Squared Error (MSE) calculations for both single-input and three-input scenarios. The outcomes are achieved through the implementation of a neural network model. The table further presents the regression values for the respective input conditions, providing insights into the predictive accuracy.

The tabulated data highlights the precision of the model's predictions for each satellite. Evidently, the MSE values for both single-input and three-input configurations are considerably low, signifying the adeptness of the neural network in capturing and modeling the intricate dynamics of the satellites' longitudinal behaviors. The regression values near 1 indicate a robust correlation between the predicted and measured values, underlining the efficacy of the neural network approach in this study.

Table 2. Comparison of Predicted vs. Measured Satellite Longitudes Differences and Their Mean Squared Errors (MSE) for Single and Three Inputs Obtained Using Neural Network

Sat name	MSE (1 input)	MSE (3 inputs)	Regression (1 and 3 inputs)
Astra-1F	8.628×10^{-4}	1.175×10^{-4}	0.99999
Eutelsat-33A	1.695×10^{-4}	1.209×10^{-4}	0.99999
Intelsat-801	1.615×10^{-3}	1.624×10^{-3}	0.99999
Meteosat-6	3.358×10^{-3}	1.067×10^{-4}	0.99999
Turksat-1B	2.858×10^{-3}	3.593×10^{-5}	0.99999
Turksat-2A	4.419×10^{-4}	1.375×10^{-5}	0.99999
Average	1.551×10^{-3}	3.364×10^{-4}	0.99999
Standard dev.	1.312×10^{-3}	6.322×10^{-4}	0.00000

This analysis demonstrates the model's consistent performance across the different satellites, further solidifying its reliability. The average MSE and standard deviation values for both input scenarios reinforce the model's accuracy and consistency.

The collective findings of this study strongly affirm the effectiveness of the employed neural network model in accurately predicting variations in satellite longitudes, thereby enriching our comprehension of decommissioned geostationary satellite behaviors in real-world scenarios. These results resonate with similar studies in the field. For instance, Ariafar and Rudiger investigated the long-term evolution of retired geostationary satellites [29]. Baresi et al. delved into the long-term evolution of mid-altitude quasi-satellite orbits, contributing to the broader understanding of orbital dynamics [30]. Proietti et al. provided insights into the long-term orbit dynamics of decommissioned geostationary satellites, aligning with the objectives of this study [31]. The confluence of these findings highlights the model's robustness and positions it within the broader context of established research endeavors, bolstering its credibility and applicability in contributing to the field's knowledge base.

In light of these findings, our study contributes to the growing body of research aimed at unraveling the intricacies of space science through advanced computational techniques. The application of time series neural networks in modeling satellite behavior displays their potential for understanding complex orbital dynamics and predicting satellite characteristics. As we continue to delve into the nuances of space phenomena, such predictive models stand to play a pivotal role in the optimal management of space assets, enhancing both the efficiency and sustainability of satellite operations.

In summary, this study represents a significant advancement in modeling the longitudinal evolution of decommissioned geostationary satellites. By employing time series neural networks, we have established a robust framework for accurately predicting satellite behavior, thereby contributing to our understanding of orbital dynamics and facilitating effective space asset management.

The successful modeling of decommissioned geostationary satellites' longitudinal evolution using time series neural networks carries several important benefits and implications for future space science and satellite operations. Accurately predicting satellite behavior post-decommissioning provides valuable insights for mission planning and decision-making. Operators can leverage the predictive model to plan end-of-life maneuvers, ensuring decommissioned satellites are safely moved to graveyard orbits, minimizing space debris generation, and optimizing resource allocation. Moreover, accurate prediction of satellite behavior post-decommissioning contributes to the sustainability and longevity of space operations by preventing satellites from becoming potential sources of space debris.

5. Conclusion

In conclusion, this study comprehensively explores the longitudinal evolution of decommissioned geostationary satellites using time series neural networks. By harnessing the power of advanced computational techniques, we have successfully modeled the behavior of these satellites after their operational lives end. Our investigation, supported by a robust dataset extracted from publicly available sources, highlights the intricate relationship between orbital dynamics and satellite longitudinal variations. The predictive capabilities of our neural network model offer significant benefits for space science, satellite operations, and the broader aerospace industry. Our findings demonstrate that accurate predictions of satellite behavior post-decommissioning contribute to enhanced mission planning, resource optimization, and effective space debris mitigation.

The successful modeling of decommissioned satellite behavior contributes to the scientific community and the responsible stewardship of our celestial environment. With each accurate prediction, we move closer to ensuring the harmony of human activities in space with preserving the space environment for generations to come.

References

- [1] Soop EM. Introduction to geostationary orbits 1993: ESA.
- [2] Oz I. Coverages stabilization of an inclined orbit communication satellite with two axis biases. *Journal of the Faculty of Engineering and Architecture* 2022; 38:1, pp. 219-230.
- [3] Oz I, Yilmaz UC. Determination of coverage oscillation for inclined communication satellite. *Sakarya University Journal of Science* 2020; 24(5), 973-983.
- [4] ITU Radiocommunication Sector: Regulations and procedures for space radio communication, Recommendation ITU-R S.1003-1, 2021.
- [5] Inter-Agency Space Debris Coordination Committee (IADC): IADC Space debris mitigation guidelines. 2007; Issue 3.0.
- [6] European Space Agency (ESA): Space debris mitigation handbook. *ESA Bulletin*, 2005; Issue 123.
- [7] Büyükkeçeci M, Okur MC. A comprehensive review of feature selection and feature selection stability in machine learning. *Gazi University Journal of Science*, 2024; 1-10.
- [8] Ameur T, Eddine A, Benalia A. ANN identification technique and fuzzy pi control of a hybrid indirect matrix converter with a flying capacitor three level inverter in power active filtering application. *Gazi University Journal of Science*, 2023;1-10.
- [9] Seymen OF. et al. Customer churn prediction using ordinary artificial neural network and convolutional neural network algorithms: a comparative performance assessment. *Gazi University Journal of Science*, 2023.

- [10] Erdem OE, Kesen SE. Estimation of Turkey's natural gas consumption by machine learning techniques. *Gazi University Journal of Science* 2020; 33.1: 120-133.
- [11] Rayan, AB, Artuner H. LSTM-Based deep learning methods for prediction of earthquakes using ionospheric data. *Gazi University Journal of Science* 2022; 35.4: 1417-1431.
- [12] Wickramasinghe L, Ekanayake P, Jayasinghee J. Machine learning and statistical techniques for daily wind energy prediction. *Gazi University Journal of Science* 2022; 35.4: 1359-1370.
- [13] Alshari H, Odabas A. Machine learning model to diagnose diabetes type 2 based on health behavior. *Gazi University Journal of Science* 2022;35.3. 834-852.
- [14] Tombaloğlu B, Erdem H. Turkish speech recognition techniques and applications of recurrent units (LSTM and GRU). *Gazi University Journal of Science* 2021;34.4: 1035-1049.
- [15] Montenbruck O, Gill E. *Satellite orbits: models, methods, and applications*, Springer 2011.
- [16] Li HN. *Geostationary satellite collocation*, Springer 2010.
- [17] Piani S. *Analytical model for propagation of debris clouds in geostationary orbit*. Tesi di Laurea Magistrale in Space Engineering, Ingegneria Spaziale. 2022.
- [18] Thomas R, Linares R. A survey of longitudinal-shift maneuvers performed by geosynchronous satellites from 2010 to 2021, 2022; 73rd Astronautical Congress, Paris, France.
- [19] CarvalhoMoraes SJP, Prado A. Analysis of the orbital evolution of space debris using a solar sail and natural forces. *Advances in Space Research* 2022; v 70(1), 125-143.
- [20] Byoung-Sun L. East–West station-keeping maneuver strategy for COMS satellite using iterative process. *Advances in space research* 2011; 47.1: 149-159.
- [21] <https://www.space-track.org/> last access March 2023.
- [22] Stepišnik T. Machine learning for effective spacecraft operation: Operating INTEGRAL through dynamic radiation environments. *Advances in Space Research* 2020; 69.11: 3909-3920.
- [23] Thomas R, Soleraa HE, Linares R. Geosynchronous satellite behavior classification via unsupervised machine learning. In 9th Space Traffic Management Conference. Austin, 2023; TX (Vol. 3).
- [24] Roberts T. *Geosynchronous Satellite Maneuver Classification and Orbital Pattern Anomaly Detection via Supervised Machine Learning*. Diss. Massachusetts Institute of Technology, 2021.
- [25] Solera HE, Linares R. Geosynchronous satellite pattern of life node detection and classification, 9th Space Traffic Management Conference, Austin TX, 2023.
- [26] Çelikel R, Gündoğdu A. ANN-based MPPT algorithm for photovoltaic systems. *Turkish Journal of Science and Technology* 202; 15.2: 101-110.
- [27] Toraman S, Turkoglu I. A new method for classifying colon cancer patients and healthy people from FTIR signals using wavelet transform and machine learning techniques. *Journal of the Faculty of Engineering and Architecture of Gazi University* 2020;35.2: 933-942.
- [28] Dogan F, Turkoglu I. Derin öğrenme modelleri ve uygulama alanlarına ilişkin bir derleme. *Dicle Üniversitesi Mühendislik Fakültesi Mühendislik Dergisi* 2019;10.2: 409-445.
- [29] Ariafar S, Rüdiger J. Long-term evolution of retired geostationary satellites. 4th European Conference on Space Debris, 2005; Vol. 587.
- [30] Baresi Net al. Long-term evolution of mid-altitude quasi-satellite orbits. *Nonlinear dynamics*, 2020; 99: 2743-2763.
- [31] Proietti S et al. Long-term orbit dynamics of decommissioned geostationary satellites. *Acta Astronautica* 2021;182: 559-573.